Proceedings of the 19th International Symposium on the Packaging and Transportation of Radioactive Materials
PATRAM 2019
August 4-9, 2019, New Orleans, LA, USA

MODELING COMPARISONS WITH AN ABOVEGROUND DRY CASK SIMULATOR

Marta Galbán
ENUSA Industrias Avanzadas S.A., S.M.E

Miriam Lloret
ENUSA Industrias Avanzadas S.A., S.M.E

Julio Benavides
Universidad Politécnica de Madrid

Gonzalo Jiménez
Universidad Politécnica de Madrid

Samuel Durbin
Sandia National Laboratories

ABSTRACT

The performance of commercial nuclear spent fuel dry storage casks is evaluated through detailed analytical modeling of the system´s thermal performance. Therefore, a thermal modeling subcommittee has been created in the Extended Storage Collaboration Program (ESCP), which consists of different phases.

The purpose of Phase I was to produce validation-quality data that can be used to test the accuracy of the modeling presently used to determine cladding temperatures in modern vertical dry casks. To produce these data sets under well-controlled boundary conditions, the dry cask simulator (DCS) was built at Sandia National Laboratories to study the thermal-hydraulic response of a single boiling water reactor (BWR) fuel assembly under a variety of heat loads, internal vessel pressures, and external configurations.

In this paper, the modeling results of ENUSA-UPM are compared to a select set of the DCS tests. An explicit model has been created using STAR-CCM+, a computational fluid dynamics (CFD) code, and representing fuel rods and water rods in the assembly in detail, which results in the advantage of the cladding temperature for every rod being calculated discretely. To define the test boundary conditions, the basic geometry, and material properties, a handbook with the required information was provided by Sandia National Laboratories.

The results for a selected number of cases (5 kW for 100 kPa and 800 kPa; 0.5 kW for 100 kPa and 800 kPa) show good agreement with the experimental data, with a maximum relative peak cladding temperature (PCT) error of 3%. Note that all pressures are absolute.

Regarding the air mass flow rate results, a maximum relative error of 10% compared to the test measurements is obtained, except for the low pressure (100 kPa) and low power (0.5 kW) cases, where the relative error is higher (20%). This increased error is likely related to the high sensitivity observed in setting the inlet boundary condition as a jump in air pressure.

1. INTRODUCTION

The purpose of the Aboveground Dry Cask Simulator (DCS) test was to provide data set that can be used to test the validity of the modeling presently used to determine cladding temperatures in vertical dry storage casks. To produce these data sets under well-controlled boundary conditions the DCS was built at Sandia National Laboratories to study the thermal-hydraulic response of fuel under a variety of heat loads, internal vessel pressures, and external configurations. In this work 4 cases have been simulated for different helium pressure vessel and powers: 100 kPa and 5 kW; 100 kPa and 0.5 kW; 800 kPa and 5 kW; and 800 kPa and 0.5 kW.

In Figure 1 the general design of the Aboveground DCS is represented. It consists of a single 9×9 boiling water reactor (BWR) fuel assembly deployed inside of a representative storage basket and a cylindrical pressure vessel that represents the canister filled with helium. Externally to the canister, air flow is buoyantly induced in the annulus between the canister and the outer shell. The four air inlets at the bottom part of the DCS have honeycomb elements inserted to straighten the flow, see [1].

The 9×9 BWR fuel assembly has 74 rods, 66 full length and 8 partial length rods with two water rods.

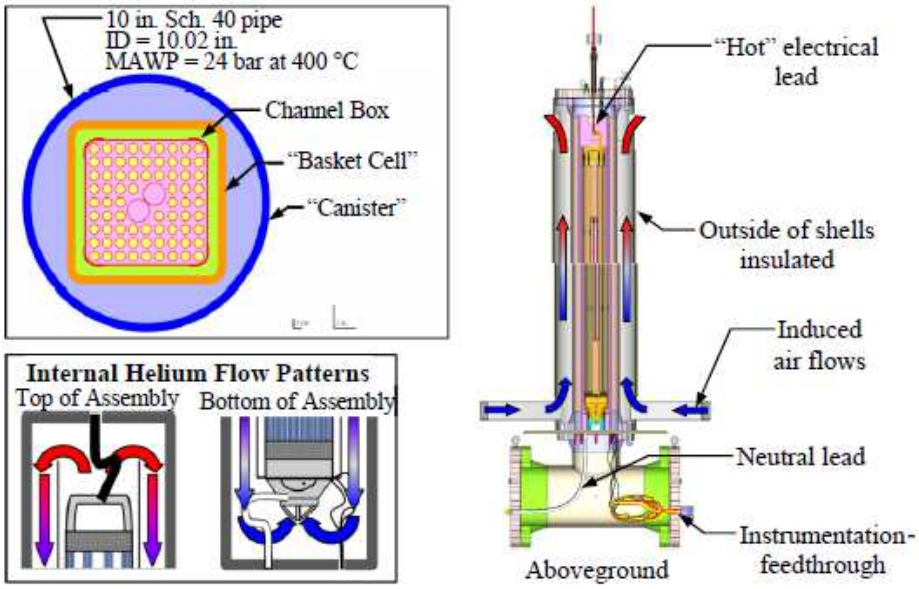

Figure 1. Aboveground DCS general design (right), plan view (upper left) and internal helium flow (lower left)

2. MODEL DESCRIPTION

To simulate this DCS test, an explicit model has been created using STAR-CCM+ version 13.02.011, a computational fluid dynamics (CFD) commercial code. CFD codes use finite volume numerical methods that solve an integral form of the fluid governing equations for mass, momentum, and energy using body-fitted meshes. For more information about STAR-CCM+ CFD, see [2].

The mesh of the simulation model extends from the cladding of each rod to the outer shell (see Figures 2 and 3).

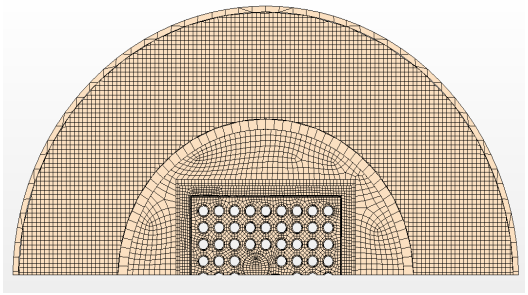

Figure 2. STAR-CCM+ explicit model

Figure 3. STAR-CCM+ explicit model ¼ symmetry mesh

2.1 APPROXIMATIONS AND TREATMENTS

To reduce computational cost and modeling efforts, approximations and additional hypothesis have been applied to the DCS model.

As the model is symmetric, half of the geometry has been modeled to reduce meshing and modeling efforts. Invoking symmetry leads to a decreased number of cells in the mesh and directly reduced computational cost.

The test assembly has been modeled starting at the inner cladding and extends to the outer shell. Each fuel rod and water rod are modeled as hollow cylinders, see Figure 4. Heat flux is applied at the inner face of the cladding. Helium flow is calculated inside the water rods and interstitial spaces between the fuel rods. The spacers were not simulated due to the additional computational cost.

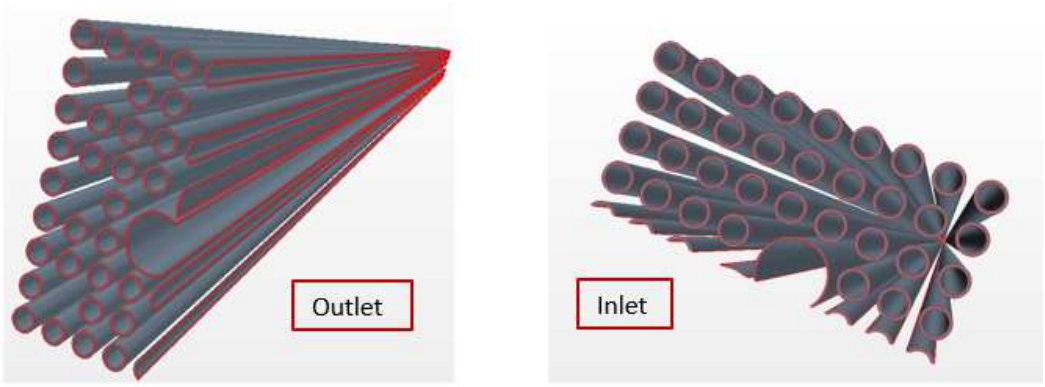

Figure 4. Model partial and full length rods

2.2 STRUCTURES AND BOUNDARY CONDITIONS

A detailed structure of the model in STAR-CCM+ is represented in Figure 5. The outside vessel Heat Transfer Coefficient (HTC) has been obtained from correlations and takes into account the radiation with the environment. The top and bottom of the canister have been considered adiabatic (as insulated walls), as suggested in the test specifications.

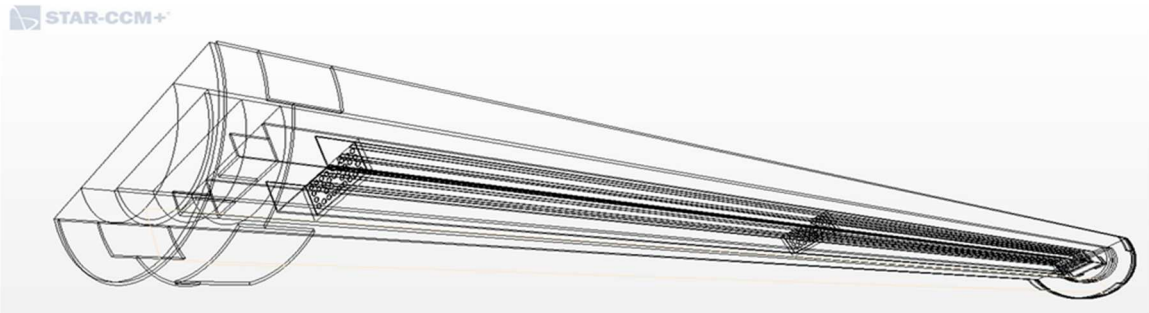

Figure 5. Detailed DCS modeling structure

For boundary conditions, pressure outlets have been defined and the inlet honeycomb elements have been modeled as a pressure jump between air inlets/outlets (stagnation inlet) calculated on the basis of data provided by Sandia National Laboratories [1].

The flow regime inside the DCS has been estimated to be turbulent, and therefore it has been modeled as RANS turbulent model: the Realizable K- ε (Shear Driven), chosen by taking into account sensitivity studies done by ENUSA Industrias Avanzadas S.A., S.M.E and UPM for other containers [3].

The physical and numerical models used in the simulation are summarize in Table 1.

Table 1 STAR-CCM+ physical and numerical scheme

STAR-CCM+ physical and numerical scheme	
Pressure-velocity coupling	Coupled flow and energy
Discretization	2nd order
Time discretization	Steady State
Gas model	Ideal gas (helium, air)
Solid material properties	Defined in the DCS handbook
Thermal properties	Variable with temperature (for both fluids and solids)
Turbulence model	Realizable k-ε (Shear Driven)
Wall function	Two layer all y+ wall treatment
Radiation model	S2S
Reference pressure	83.3 kPa (Ambient pressure in Albuquerque, NM)
Mesh	Directed Mesh + Automated Mesh

3. RESULTS

Results obtained for the four cases simulated (0.5 kW and 100 kPa; 5 kW and 100 kPa; 0.5 kW and 800 kPa; and 5 kW and 800 kPa) using the model described in this work are included in this section.

In Tables 2 and 3 air mass flow rate and peak cladding temperature (PCT) results obtained for the four simulations compared to the test results are summarized.

Table 2 Air mass flow rate results

Power (kW)	Pressure (kPa)	Test air mass flow rate (kg/s)	ENUSA-UPM air mass flow rate (kg/s)	Absolute air mass flow rate error (kg/s)	Relative air mass flow rate error (%)
5	800	0.0660	0.0600	0.006	9.1
5	100	0.0721	0.0642	0.008	11.0
0.5	800	0.0243	0.0252	0.001	3.5
0.5	100	0.0288	0.0215	0.007	25.5

Regarding air mass flow rate results in Table 2, the minimum difference between test measurements and simulation results are for the low power (0.5 kW) and high pressure (800 kPa) case with a relative error of 3.5%.

In a previous simulation, the error obtained for the low power (0.5 kW) and high pressure (800 kPa) case gave an error of 80%, so reviewing and improving this simulation was one of the first goals. After checking different parameters including boundary conditions and meshing, the air pressure differential between the pressure inlet and pressure outlet (both initially set to 0 Pa absolute) was found to be incorrect. Although the code calculates hydrostatic pressure in the computational domain, the boundaries do not compensate for the hydrostatic pressure. This results in certain downward flow from the outlet to the inlet (if the vessel had not been heated the flow would flow from outlet to inlet). This can be fixed by initializing the pressure inlet with a pressure of 4.4 Pa (approximately the hydrostatic pressure), with this the 800 kPa and 5 kW case went from an error of 80% in mass flow to a more reasonable value of 3.5%.

In Table 2, the low power (0.5 kW) and low pressure (100 kPa) case relative error is approximately 25%. It should be noted that this result corresponds to the value obtained before the correction of the pressure inlet explained in the previous paragraph had been taken into account. The results are expected to improve by introducing this pressure inlet in the simulation.

Table 3 PCT results

Power (kW)	Pressure (kPa)	PCT axial level (m)	Test PCT (K)	ENUSA-UPM PCT (K)	Absolute PCT error (K)	Relative PCT error (%)
5	800	3.93	659.00	648.26	10.7	1.6
5	100	1.05	716.00	737.14	21.1	3.0
0.5	800	4.00	359.00	358.05	0.9	0.3
0.5	100	1.94	376.00	380.10	4.1	1.1

In Table 3, PCT results show good agreement with experimental measurements yielding a maximum relative error of 3% for the high power (5 kW), low pressure (100 kPa) case. Due to setting an air pressure jump, the PCT results are relatively unaffected compared to the effect on air mass flow rate. When setting a pressure at the inlet, the relative error in PCT improved from 2.6% to 0.3% for the 800 kPa and 0.5 kW, as shown in Table 3.

In Figure 6, the temperature distributions for the 0.5 kW and 800 kPa and 5 kW and 800 kPa cases are presented.

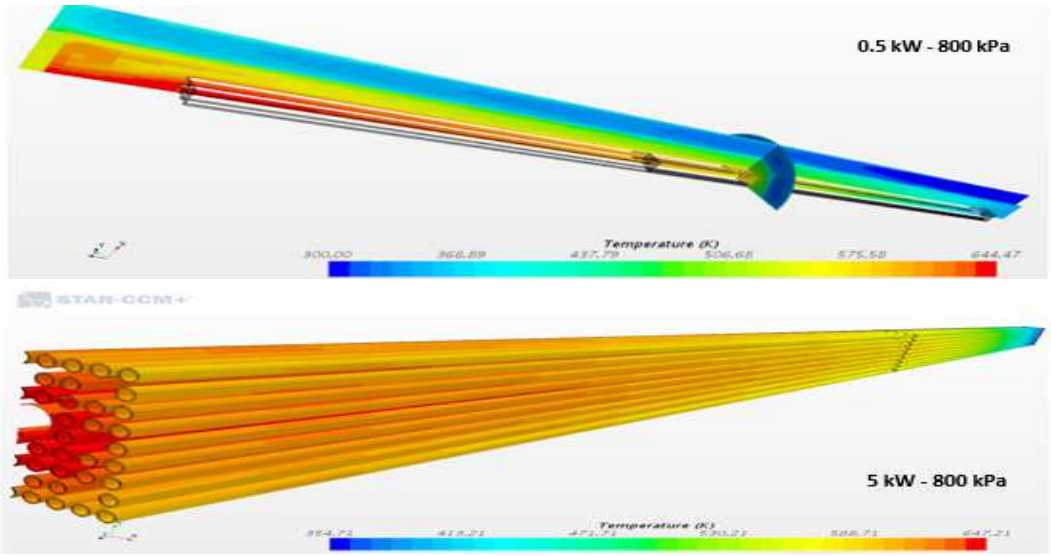

Figure 6. Temperature distributions (K)

In Figures 7 and 8, flow velocity vectors are represented at the inlet of the DCS, outlet and at the mid-height of the cask, respectively, for the 0.5 kW and 800 kPa case. As can be seen in the Figures, air flow enters through the honeycomb elements, modeled as a pressure jump, and rises up the height of the cask via natural convection to the outlets at the top of the cask where it exits at a higher temperature and velocity. It also can be seen that the flow near the canister is at higher velocity than the air next to the shell wall.

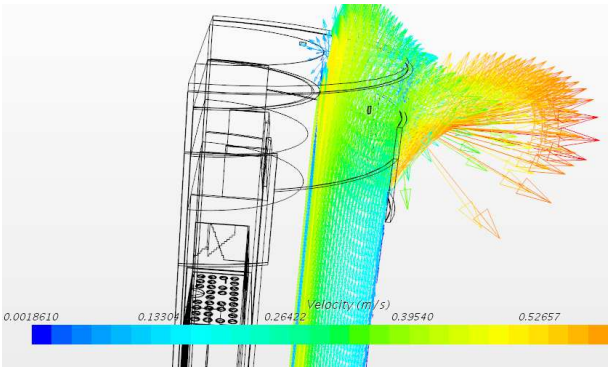

Figure 7. Flow velocity vectors outlet (m/s)

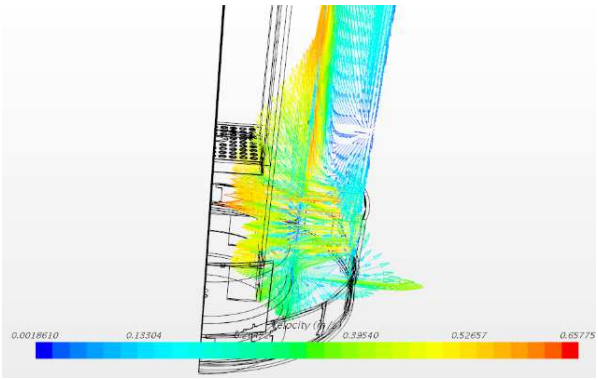

Figure 8. Flow velocity vectors inlet (m/s)

Due to paper extent limits, only the most representative results have been included in this section. Figures 9 and 10 represent the maximum and average fuel temperature results obtained for 0.5 kW and 800 kPa and for 5 kW and 0.5 kW for 100 kPa cases compared to experimental results. Temperature profiles show good agreement, with a maximum difference of 9 K between the model and experiment results for Figure 9. Temperature comparisons to the experiment in Figure 10, show slight deviations in the modeling results at the top of the fuel axial level, which is directly related to the top of the canister being considered adiabatic and will be discussed later. All four cases present this approach, with the 5 kW and 100 kPa case showing the largest discrepancy.

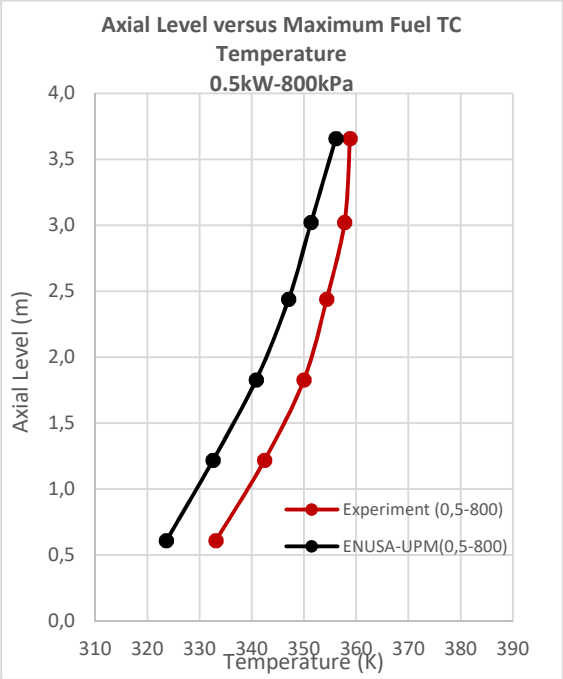

Figure 9. Maximum Fuel Temperature (K)

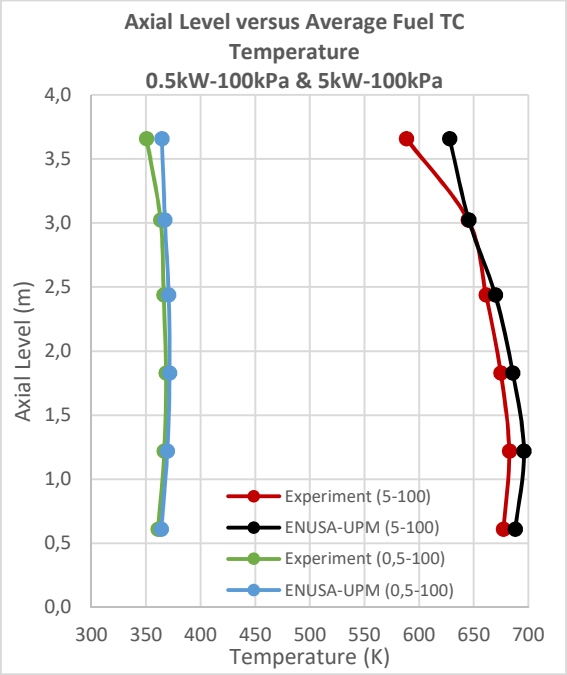

Figure 10. Average Fuel Temperature (K)

In Figures 12 and 13 temperatures on the other structures of the test assembly such as the basket and the outside shell are shown. Both Figures show the same behavior between the model results and the thermocouple (TC) measurements with differences at the top of the fuel axial level related to the adiabatic assumption made for these cases. Despite these differences, the results show good agreement between model results and measured data.

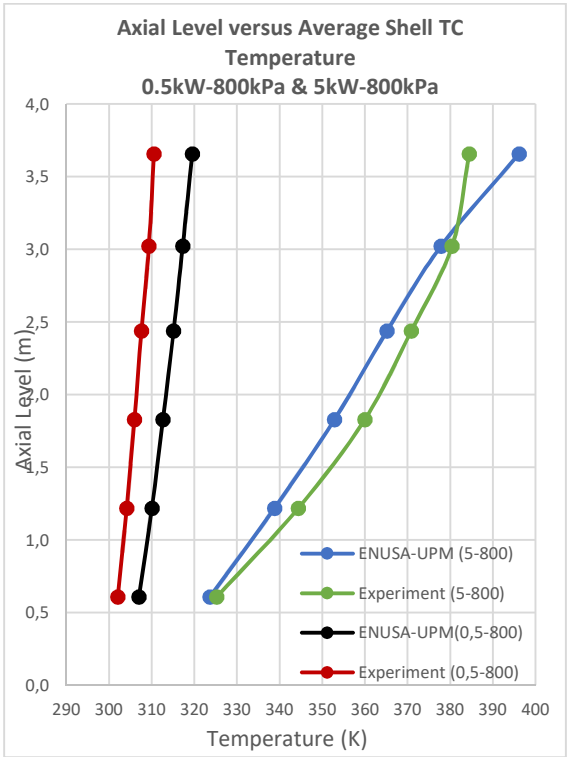

Figure 11. Average Shell Temperature (K)

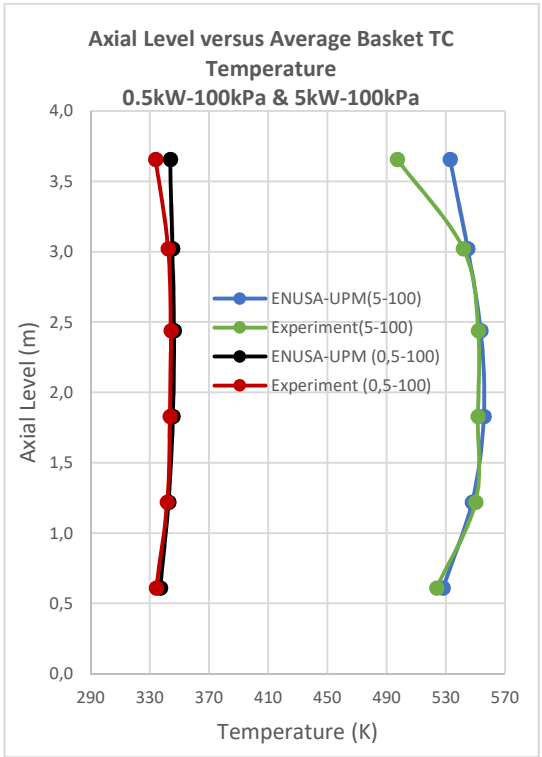

Figure 12. Average Basket Temperature (K)

Model to experiment comparisons included in Figures 14 and 15 show the deviations detected between ENUSA-UPM model and the test measurements.

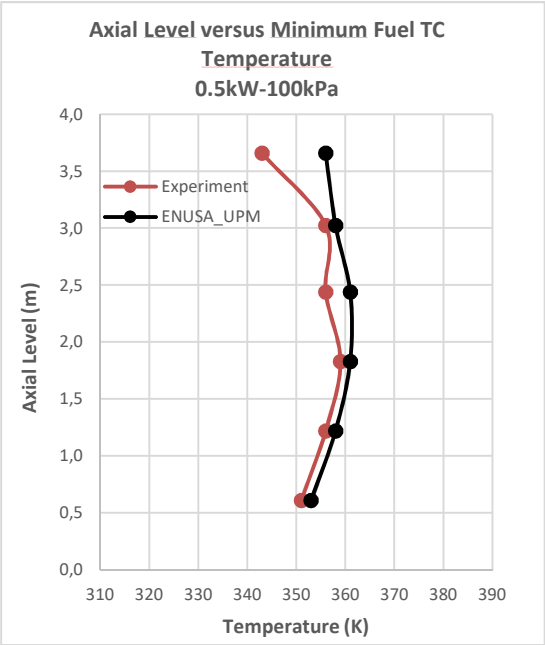

Figure 13. Minimum Fuel Temperature (K)

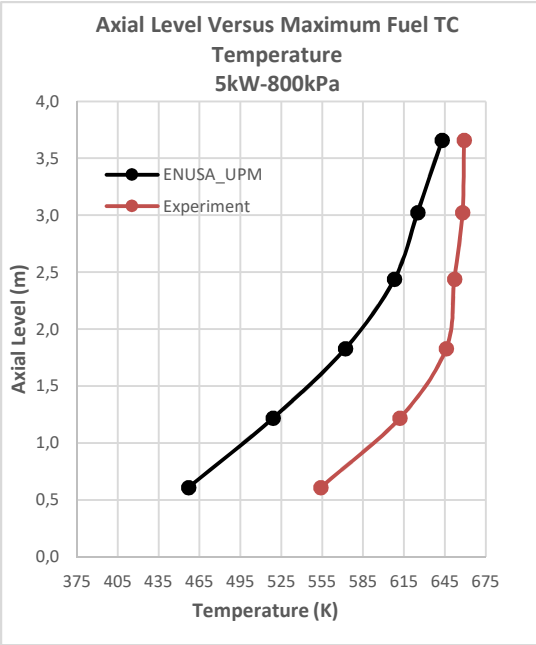

Figure 14. Maximum Fuel Temperature (K)

Temperature comparisons to the experiment given in Figure 14 show a slight deviation in the modeling results at the top of the fuel axial level, which is directly related to the top of the canister being considered adiabatic due to an insulated wall (as stated in the DCS Handbook, [2]). This approach has proven to significantly underestimate heat transfer near the top of the assembly. This can be seen in the rest of the cases, which is most evident for the high power (5 kW) cases.

Figure 15 shows a large discrepancy between the experiment and the simulation model. One hypothesis for this discrepancy is that treating the helium as an ideal gas at high pressures might not be correct and lead to the significant error shown above. The absence of the spacers in the assembly might offer another explanation for the differences found between the model and the experiment data. Future work is needed to test these hypotheses.

4. CONCLUSIONS

In this work, it is shown that realistic results for PCT and overall temperature distribution using CFD calculations can be obtained successfully. Nonetheless, there is still work to be done. The simulation results have good agreement with the test measurements as can be seen in Figures 9 to 12. Peak cladding temperatures in particular as seen in Table 3 show good agreement, where the maximum relative error is 3% for the high power (5 kW) and low pressure (100 kPa) case.

One of the main advantages of using an explicit model is the ability to obtain the cladding temperature on a rod-by-rod basis in the simulation. Cladding temperature is a key parameter

to prevent unacceptable cladding degradation during storage, such as creep and hydride reorientation that can appear at high cladding temperatures. This detailed approach also allows the use of fewer assumptions, such as fixing a thermal conductivity or a pressure drop in the fuel area. As a disadvantage, creating an explicit model requires more work regarding meshing and geometry modeling for the user.

As main areas for improvement, sensitivity studies for turbulence models that have been done for other works (see [3]). In addition, addressing compressibility issues for the helium gas model at high pressures and introducing the spacers in the model are some areas of interest for further exploration.

5. REFERENCES

[1] E.R. Lindgren and S.G. Durbin, Sandia National Laboratories. November 30, 2017. MATERIALS AND DIMENSIONAL REFERENCE HANDBOOK FOR THE BOILING WATER REACTOR DRY CASK SIMULATOR.

[2] SIEMENS, 2018. STAR-CCM+ 13.02 USER GUIDE.

[3] Benavides, J., Jimenez, G., Galbán, M., Lloret, M., 2018. STAR-CCM+ SIMULATION OF A SPENT FUEL DRY CASK EXTERNAL COOLING BY NATURAL CONVECTION. TopFuel Prague Sept. 2018.